

Cellulose with Bidentate Chelating Functionality: An Adsorbent for Metal Ions from Wastewater

Abdalahdi Deghles,^{a,*} Othman Hamed,^{b,*} Mai Azar,^b Bahia Abu Lail,^b Khalil Azzaoui,^c Ahmad Abu Obied,^b and Shehdeh Jodeh^b

A cellulose derivative with multiple coordination sites for metals composed of cellulose powder and 1,2-phenylnediamine was synthesized and evaluated as an adsorbent for metal ions from wastewater. The cellulose powder was generated from the solid waste of the olive industry. The adsorption efficiency of the cellulose amine polymer toward Fe(III) and Pb(II) was investigated as a function of adsorbent dose, temperature, pH, and time. The adsorption parameters that lead to excellent adsorption efficiency were determined. In addition, the polymer showed an excellent extraction efficiency toward approximately 20 metal ions present in a sewage sample. The cellulose amine derivative had several coordination sites that included amine, hydroxyl, and aromatic groups. The diversity and frequency of the coordination sites explained the high efficiency of the polymer for metal ions. The thermodynamic analysis results supported the spontaneous adsorption efficiency of the polymer at room temperature. The adsorption process fit well with the Langmuir adsorption isotherm model.

Keywords: Cellulose powder; Metal ion; 1,2-Phenylene diamine; Wastewater; Cellulose aldehyde; Atomic adsorption spectroscopy

Contact information: a: Graduate Studies Department, Al-Istiqlal University, Ariha, Palestinian Territories; b: Department of Chemistry, College of Science, An-Najah National University, Nablus, Palestinian Territories; c: Laboratory of Mineral Solid and Analytical Chemistry LMSAC, Department of Chemistry, Faculty of Sciences, Mohamed 1st University, P.O. Box 717;

* Corresponding authors: ohamed@najah.edu; daghlas2014@pass.ps

INTRODUCTION

There is a constantly increasing demand for more sources of fresh water to cover the growing need for food production and human activities (Milieu 2010). Recycling the wastewater released from both industrial and human activities could be an answer for this demand. Wastewater contains a wide variety of toxic materials, both organic and inorganic, depending on the discharging source (Gupta *et al.* 2015; Hokkanen *et al.* 2016). These materials are harmful to plants and animals (Gupta and Babu 2009). The inorganic pollutants include toxic metal ions that are discharged mainly from medical activities, agriculture, plumbing, household chemicals, body care products, and other industrial activities. Some of the toxic metal ions that raise a serious concern are Cd²⁺, Cu²⁺, Mn²⁺, Mg²⁺, Sr²⁺, Al³⁺, Co²⁺, Ni²⁺, Cr³⁺, Zn²⁺, and Pb²⁺ ions (Sud *et al.* 2008).

Purifying the wastewater from toxic heavy metals is performed by several reported methods, and among these, adsorption is the most applicable (Qaiser *et al.* 2009) and it receives the most attention because it is highly effective and low-cost (Saravanan and Ravikumar 2015). Among the most effective metal adsorbents is activated carbon. However, it is not optimal in some cases due to the high processing costs (O'Connell *et al.*

2008). Additionally, natural-based materials, such as clay, zeolites, and peat, are among the most evaluated materials as adsorbents for toxic heavy metal ions from wastewater (Adeyemo *et al.* 2017; Chwastowski *et al.* 2017; Uddin 2017; Bo *et al.* 2018; Lin *et al.* 2018). They are the most attractive because they are renewable and available at a relatively low cost (Jodeh *et al.* 2018; Moa *et al.* 2018). In addition, other natural products, such as cellulosic materials, lignin, chitosan, and hemicelluloses, received a lot of attention. Several cellulosic-based adsorbents, such as kenaf, cotton linters, wheat straw, wood sawdust, and rice husk, were prepared and investigated as an adsorbent for toxic heavy metal ions such as those mentioned above (Nada *et al.* 2002; Acar and Eren 2006; Karnitz, Jr. *et al.* 2007; Doan *et al.* 2008; Gupta and Babu 2009; Nagy *et al.* 2013; Vieira *et al.* 2014; Muhammad *et al.* 2018). Cellulose nanoparticles (CNC) are promising adsorbent for heavy metal ions (Zelić *et al.* 2018). Despite all of the rapid progress in the study of natural-based metal adsorbents, many natural-based materials and their derivatives have not been explored as an adsorbent for metal ions.

This work focused on a cellulose powder derivatized with a bidentate chelating agent as a potential new adsorbent for metal ions. The cellulose powder was extracted from solid waste from the olive industry and was reacted with a bifunctional aromatic amine in a three-step process that involved the oxidation of cellulose to aldehyde, the conversion of oxidized cellulose to imine, and the reduction of the imine to an amine. The bifunctional aromatic amine chosen for this purpose is 1,2-phenylenediamine. The positions of the amino groups (ortho) in addition to the presence of other functional groups (hydroxyl, ether, and aromatic in the target cellulose derivative) makes it a novel adsorbent for metal ions. The prepared cellulose amine polymer (cell-o-PDAm) was evaluated as an adsorbent for Fe(III) and Pb(II) from water and other metal ions from a real sample of wastewater. To the best of our knowledge, the cell-o-PDAm presented in this work is the first example in the literature of cellulose polymer with an aromatic amine bidentate ligand.

EXPERIMENTAL

Materials

All reagents used in this study were purchased from Sigma-Aldrich (Jerusalem, Israel) and used as received. The olive industry solid waste (OISW) used in this work was obtained from an olive factory located in city of Tulkarm, Palestine.

Cellulose aldehyde

A solution of sodium hydroxide (8% by weight) was prepared by dissolving 8.0 g of sodium hydroxide in 92.0 mL distilled water. To it was added 6.0 g of cellulose powder. The produced mixture was stirred for 20 min, diluted with water, filtered, and washed several times with distilled water. Then the mixture was neutralized *via* dropwise addition of the diluted solution of acetic acid (2% by weight) and washed again with water. A sample of the produced activated cellulose (5.0 g, 0.031 mol/anhydroglucose repeat unit (AGU)) was added to a beaker, followed by suspended it in 150.0 mL of distilled water. The flask containing the cellulose suspension was completely wrapped with aluminum foil to isolate it from light. Sodium periodate (12.8 g, molecular mass (MM) = 213.9 g/mol, 0.06 mol) was added to the cellulose suspension in two portions, 6.4 g each at 6 h intervals. The reaction mixture was stirred at 40 °C for approximately 12 h. The produced cellulose aldehyde was collected *via* filtration and washed with water (3 × 250 mL). Aldehyde

content (1.89/AGU) was determined according to a previously reported procedure (Kim *et al.* 2000).

Cellulose o-phenylenediamine polymer

Cellulose aldehyde (2.0 g, 0.012 mmol of AGU) and ethanol (40 mL) were added to a round bottom flask (100-mL) fitted with a magnet stir bar and a reflux condenser. Next, 1,2-diaminobenzene (1.3 g, 12.4 mmol) was added to the suspension. The reaction was refluxed for approximately 3 h. The reaction mixture was cooled to room temperature, and sodium borohydride (0.3 g) was added to the suspension. The reaction mixture was stirred at room temperature for 8 h. It was then treated with a solution of ammonium chloride (0.5%) to destroy excess sodium borohydride. The produced cellulose amine polymer was collected through suction filtration and first washed with water, then ethanol, and then air dried.

Methods

Characterization

The Fourier transform infrared (FTIR) spectra were recorded on a Nicolet 6700 FTIR spectrometer (Thermo Fisher Scientific, Waltham, MA, USA) equipped with the Smart Split Pea™ Hemi Micro ATR accessory (International Crystal Laboratories, Garfield, NJ, USA). The following parameters were used: resolution was 4 cm⁻¹, spectral range was 600 cm⁻¹ to 4000 cm⁻¹, and number of scans was 128. The surface morphology of the cellulose polymer and derivatives were examined using scanning electron microscopy (SEM) (S-4800; Hitachi, Tokyo, Japan) at an acceleration voltage of 3.0 kV after sputter coating the sample with gold (Cressington Sputter Coater; Ted Pella, Inc., Redding, CA, USA). The metal ion analysis was performed using inductively coupled plasma mass spectrometry (ICP-MS) *via* an iCAP™ RQ ICP-MS (Thermo Fisher Scientific, Waltham, MA, USA).

Adsorption study

This work followed a batch adsorption experiment. All experiments were performed in a glass container (50-mL) that was placed in a water bath equipped with a shaker. Different variables on the polymer efficiency for metal adsorption (*e.g.*, metal ion concentration, pH values, adsorbent dosage, adsorption time, and temperature) were examined. The adsorption study was performed on the two metal ions Pb(II) and Fe(III). After each adsorption run, a sample from the mixture was collected *via* filtration through a 0.45-μm syringe filter and subjected to a flame atomic adsorption analysis at 193.7 nm to determine the residual metal ions concentration. All adsorption experiments were performed in triplicate, and the mean of the three runs was reported. The adsorbent efficiency and the amount of metal ions adsorbed by the cell-o-PDAm adsorbent q_e (mg/g) was determined according to Eqs. 1 and 2, respectively,

$$R (\%) = \frac{C_0 - C_e}{C_0} \quad (1)$$

$$Q_e = \frac{C_0 - C_e}{m} V \quad (2)$$

where C_0 and C_e are the initial and equilibrium concentrations (ppm) of metal ion in solution, respectively, Q_e is the equilibrium adsorption capacity (ppm), m is the mass of cell-o-PDAm (mg), and V is the volume of the solution (L).

Wastewater purification

A sample of sewage water was collected from the sewage system (Nablus, Palestine) and used in this study. The sample was subject to analysis using ICP-MS (performed by the Water Center at An-Najah National University, Nablus, Palestine) to determine the metals' content and their concentrations. A 50.0 mL sample of the sewage water was placed in an Erlenmeyer flask and its pH values were adjusted to 6.3. Each sample received 0.1 g of cell-o-PDAm. The mixture was shaken at room temperature for 30 min. A sample was withdrawn from the mixture with a syringe, pushed through a 0.45- μm syringe filter, and subjected to ICP-MS analysis for any residual metal ions concentrations.

RESULTS AND DISCUSSION

Product Analysis

The cellulose powder was extracted from olive industry solid waste following a process of pulping and bleaching, as reported in previous studies (Hamed *et al.* 2012, 2014). The produced cellulose powder was oxidized to cellulose aldehyde by reacting it with sodium periodate, following a published procedure (Kim *et al.* 2000). The reaction was performed under neutral conditions at 40 °C for 12 h. The FTIR spectrum of the oxidized celluloses is shown in Fig. 1a. The most noticeable peaks for cellulose dialdehyde (CDA) were observed at 1732 cm^{-1} , 1425, 1375, and 1140 cm^{-1} , assigned to C=O (aldehyde), CH_2 asymmetric bending, C-O stretching of ether and alcohol, and C-O-C stretching of β -glycosidic linkage, respectively. The weak band at 1732 cm^{-1} was due to the hydration and acetal formation (Lázaro-Martínez *et al.* 2010; Algarra *et al.* 2019). The mechanism is depicted in Fig. 1b.

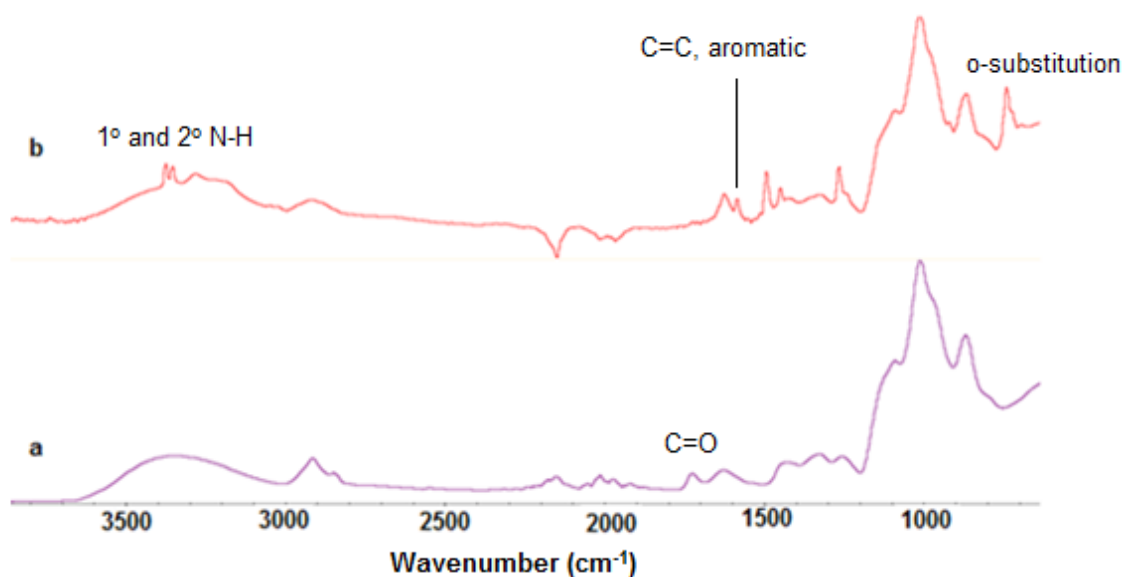


Fig. 1. (a) FTIR spectrum of cellulose aldehyde and (b) FTIR spectrum of cellulose amine

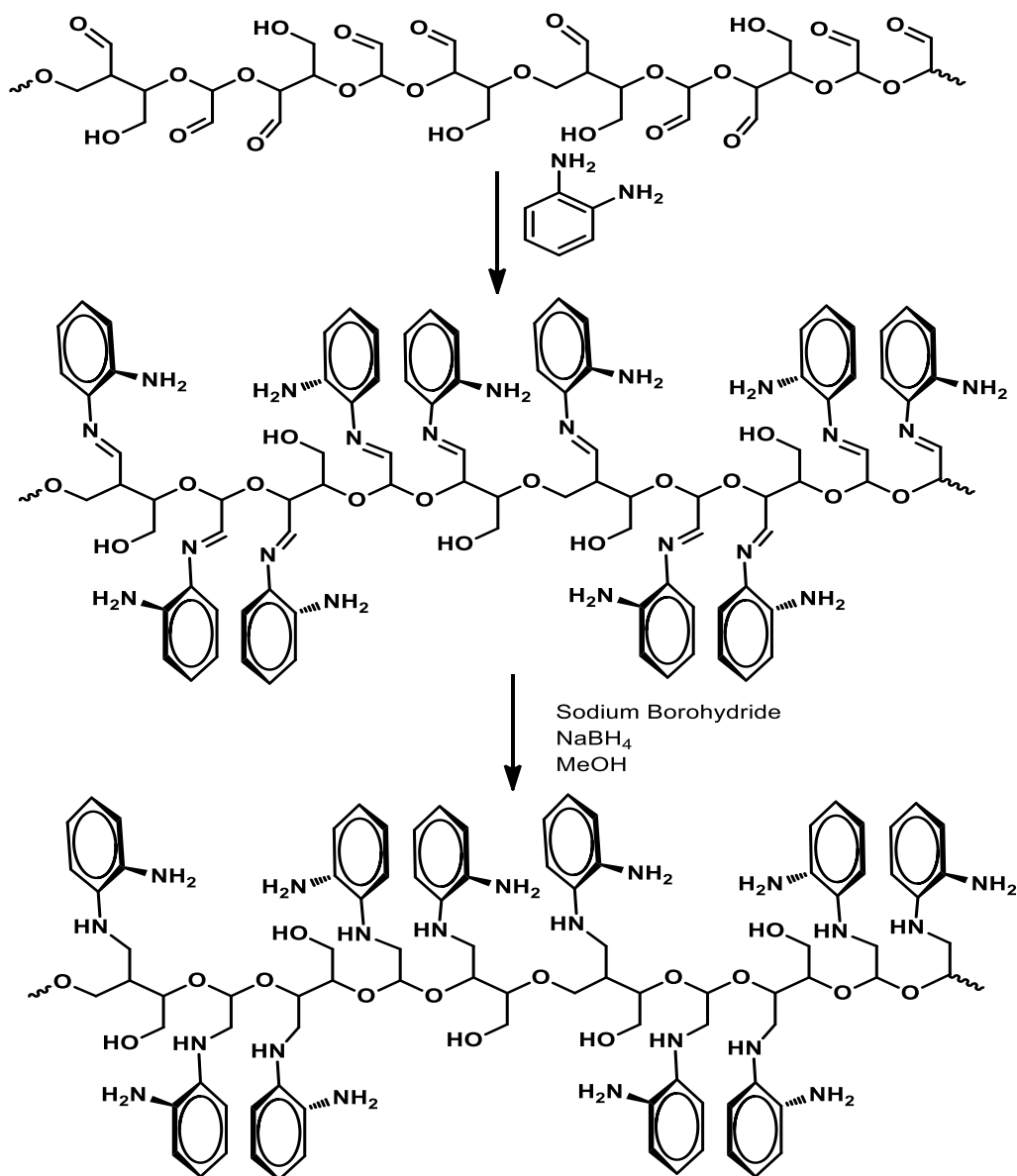


Fig. 2. Schematic showing the molecular structures of products reaction condition

The X-ray diffraction (XRD, D8 Advance; Bruker, Hamburg, Germany) patterns of cellulose aldehyde and cell-o-PDAm are shown in Fig. 1S. The intensity of the crystalline peaks at $2\theta = 16^\circ$ and $2\theta = 32^\circ$ in cellulose aldehyde broadened with some shift in their values. This could indicate a loss of crystallinity. The loss of crystallinity was attributed to the ring opening of glucopyranose, which causes a disruption and loss of H-bonding, and consequently, a loss of crystallinity (Kim *et al.* 2000; Heinze and Liebert 2001). The XRD of cell-o-PDAm showed that the cellulose crystallinity completely changed as the new compound emerged.

The aldehyde carbonyl group had an electrophilic carbon, therefore undergoing a condensation reaction with a nucleophile, such as amine, to form an imine after the loss of a water molecule. Reduction of the cellulose imine with sodium borohydride produces cellulose amine, as shown in Fig. 2. The produced amine had several coordination sites for

metal ions, including amines, hydroxyl, and aromatic functionalities. A representative molecular structure of cell-o-PDAm is shown in Fig. 2.

The FT-IR spectra of cell-o-PDAm (Fig. 1a) showed two peaks at 1635 cm^{-1} and 1610 cm^{-1} , corresponding to a primary amine and an aromatic C=C, respectively. The broad adsorption peak at approximately 3350 cm^{-1} was composed of several peaks originating from O-H or N-H stretching vibrations of primary and secondary amines. Additionally, the IR spectrum showed a peak at 2930 cm^{-1} that could have been attributed to the symmetric and asymmetric stretching vibration of the C-H bond. The peak at 750 cm^{-1} could be related to ortho substitution of phenylene diamine.

The SEM images of cellulose aldehyde, and the cell-o-PDAm prepared from it, are shown in Fig. 3.

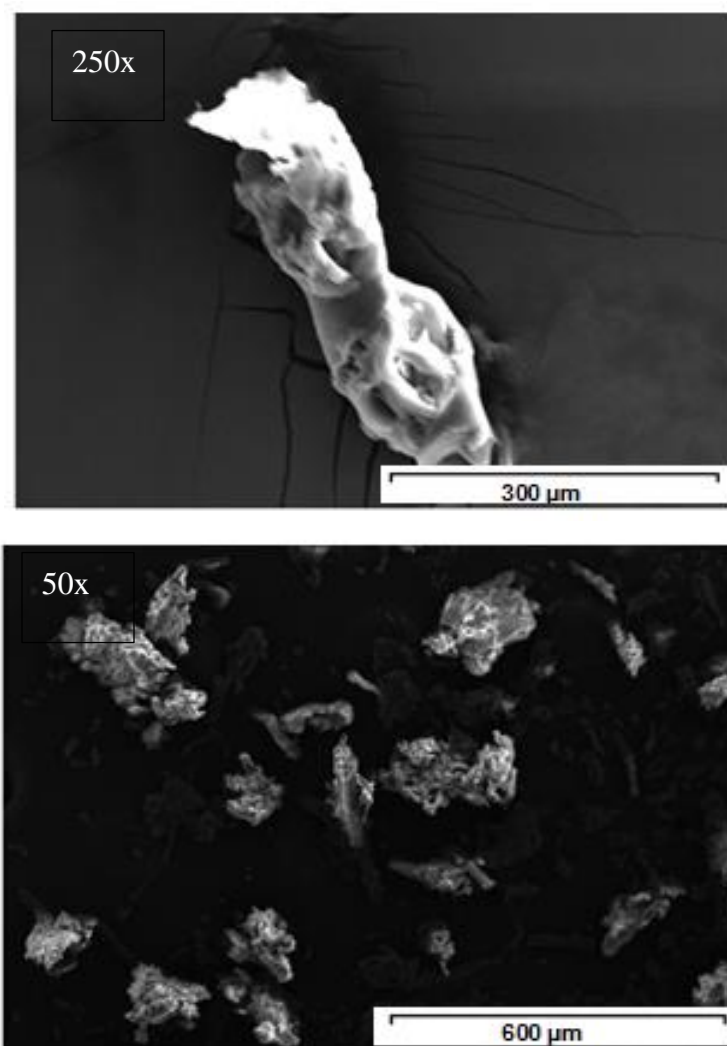


Fig. 3. SEM images of (a) cellulose aldehyde and (b) cell-o-PDAm at magnifications of 250x and 50x, respectively

The cellulose aldehyde image showed that the cell structure had been damaged. The morphology of cell-o-PDAm as shown in its image was a highly porous spongy type. The solubility of cell-o-PDAm in water was evaluated by suspending a known weight (1.00 g)

of cell-o-PDAm in water (50 mL) for approximately 12 h before being filtered and dried. It showed minimal weight loss within the experimental error.

Metal Ions Extraction

The extraction was completed using a batch adsorption process. During this process, a known weight (ranging from 0.5 mg/mL to 5.0 mg/mL metal solution) of cell-o-PDAm was suspended in an aqueous solution of metal ions, filtered, and analyzed. The analysis was performed on the filtrate to determine the concentration of the extracted ions. The effects of several variables (*e.g.*, adsorbent dosage, extraction time, temperature, and pH) were evaluated to determine the best conditions for the highest adsorption efficiency. The adsorption study was performed on lead (Pb) and iron (Fe) ions.

Optimum Adsorbent Dosage

The dosage that provided the lowest residual concentration of metal ions was chosen as the optimal dosage. This was achieved by performing the experiment with 50 mL each of Fe(III) and Pb(II), with a concentration of 30 ppm, pH value of 6.3, adsorption time of 30 min, and performed at room temperature. The effect of the adsorbent dosage on the removal of Fe(III) and Pb(II) ions is shown in Fig. 4a. As shown in the figure, the amount of metal extracted increased when increasing the polymer dosage. Metal ion removal reached approximately 67.8% and 88.1% for Pb(II) and Fe(III), respectively, at a 2.0 mg/mL dose of cell-o-PDAm. At dosages higher than 2.0 mg/mL, it became nearly constant. This was because the adsorption process was controlled by two mechanisms, diffusion and surface coordination. An increase in the dosage resulted in the number of available binding sites increasing, and thus the ion removal increased. When all sites on the surface were occupied, the diffusion process began. It is controlled by osmosis; when the concentration of the metal ions adsorbed by the polymer are equal to that of the solution, the adsorption stops (Abdel-Ghani *et al.* 2007).

Effect of Initial Ion Concentration

The effect of the initial ion concentration on the adsorption efficiency was evaluated under the following adsorption conditions: adsorption time was 30 min, adsorbent dose was 2.0 mg/mL, and pH was 6.3. The amines' functional groups were in Lewis base form at this pH value. As shown in Fig. 4b, the highest removal was at the concentration of 10 ppm. At this concentration, the percent of ions removed reached 88.3% and 83.2% for Fe(III) and Pb(II), respectively. At concentrations higher than 10 ppm, the removal started to gradually decline. The results indicated that at low concentrations of metal ions, the driving force for adsorption was controlled by the ion diffusion (Sahmoune *et al.* 2011). At high concentrations, the availability of the binding sites was the limiting factor, and the number of available sites was governed by the adsorbent dosage. According to the obtained results, at a concentration of approximately 10 ppm, the binding sites were almost saturated for this reason. However, concentrations higher than 10 ppm resulted in the rate of metal removal decreasing.

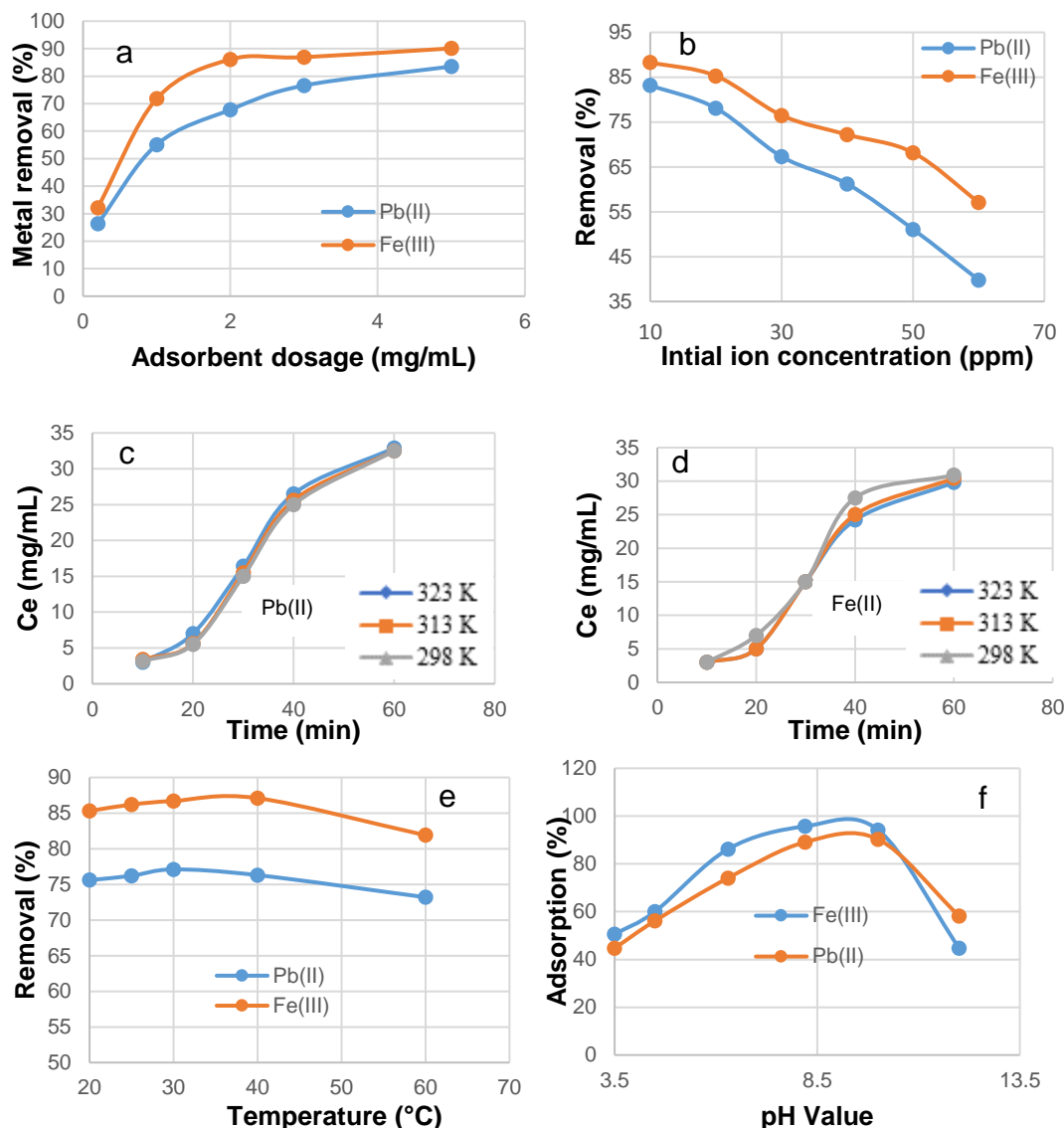


Fig. 4. Effect of (a) adsorbent dose, (b) initial ion concentration, (c) adsorption time for Pb(II), (d) adsorption time for Fe(III), (e) temperature, and (f) pH on the metal removal by cell-o-PDAm

Effect of Contact Time

Adsorption of the metal ions Pb(II) and Fe(III) by cell-o-PDAm as a function of time was evaluated under the conditions: pH 6.3, initial ion concentration of 20 ppm, adsorption temperature of 25 °C, and the adsorbent dose was 2.0 mg/mL. As shown in Figs. 4c and 4d, the adsorbed metal ions rapidly increased for the first 40 min due to the availability of the binding sites. Then, the adsorption rate became almost constant for the next 20 min and reached equilibrium after 40 min. The results indicated that at this period, almost all the coordination sites are occupied (Liu *et al.* 2013). A contact time of 40 min was chosen as the optimal contact time. The two ions showed nearly similar adsorption behavior with time.

Effect of Temperature

The effect of temperature on the adsorption of metal was evaluated under the conditions: pH 6.3, initial metal ion concentration of 30 ppm, adsorption time of 40 min, and the adsorbent dose was 2.0 mg/mL (Fig. 4e). The adsorption efficiency showed no dependence on the temperature. Up to approximately 60 °C, the adsorption efficiency was almost constant.

Effect of pH

The effect of the adsorption efficiency as a function of the pH value is shown in Fig. 4f. The pH value was a critical factor in metal adsorption because the pH value could control the surface charge of the polymer. At low pH values (≤ 3.0), the amine is in the salt form ($-\text{NR}_2\text{H}_2^+$). For this reason, the adsorption efficiency was the minimum (approximately 20%). However, at pH values higher than 3.0, the lone pair of electrons on amine N became more available, causing the amine group to behave as a metal binding agent. The highest efficiency was observed at pH 8.6. At higher pH values, the adsorption efficiency started to decline. The formation of metal oxides and metal hydroxides at pH higher than 9.0 could be the reason for the decreasing adsorption efficiency.

Wastewater Purification from Metals

A sample of wastewater was collected from a sewer system and was treated with cell-o-PDAm. A photograph of the wastewater sample before and after its treatment is shown in Fig. S2. The metal content of the sample before and after purification is summarized in Table 1.

Table 1. Metal Concentration of Wastewater before and after Treatment, pH 6.8

Metal Ion	Before (ppm)	After (ppm)	Removal (%)
Ag	38.1	0.635	98.3
Al	4680	52.2	98.9
Pb	12.5	1.6	98.7
Cu	103	0.644	62.1
Cd	0.67	0.07	89.6
Cr	523	43.1	91.8
Co	12.5	1.07	91.4
Fe	8156	383	95.3
Ga	2.4	0.48	80
Rb	35.4	20.7	41.5
Li	6.7	5.3	21
Mn	167	25.3	85
Mo	9.7	2.4	75.3
Ni	43	11	74.7
Sr	609	231	62
Cs	0.31	0.13	58.1
V	16	1.4	92
Zn	696	19.3	98

The results showed that the cell-o-PDA polymer had excellent efficiency toward most of the metals present in the wastewater sample, *i.e.*, the removal exceeded 90% for several of them.

The high efficiency of the cellulose amine polymer toward the metal ions was possibly related to the unique structure that was composed of several coordination sites that include amine, hydroxyl, and aromatic groups.

Adsorption Analysis

The Langmuir (Eq. 3) and Freundlich isotherm (Eq. 4) methods were used to evaluate the distribution of metal ions on the surface of cell-o-PDAm after reaching the equilibrium at a constant temperature (Limousin *et al.* 2007; Azzaoui and Mejdoubi 2014). The Langmuir model assumes the formation of a monolayer of adsorbate on a homogeneous surface of an adsorbent (Brdar *et al.* 2012). However, the Freundlich model describes the adsorption between the adsorbate molecule and the adsorbent with a heterogeneous surface. Below is Eq. 3,

$$\text{Langmuir isotherm model: } \frac{C_e}{Q_e} = \frac{1}{q_{\max}} C_e + \frac{1}{q_{\max} K_L} \quad (3)$$

where C_e is the equilibrium concentration of metal ion (ppm), Q_e is the amount of adsorbate adsorbed per unit mass of cellulose amine at equilibrium (mg/g), Q_{\max} is the theoretical maximum monolayer adsorption capacity of the adsorbent (mg/g), and K_L is the Langmuir isotherm constant related to the adsorption energy (L/mg). Equation 4 is as follows,

$$\text{Freundlich isotherm model: } \ln(q_e) = \ln k_f + \frac{1}{n} \ln C_e \quad (4)$$

where K_F and $\frac{1}{n}$ are empirical constants that indicate the relative adsorption capacity and intensity related to the affinity of the metal, respectively.

The Langmuir isotherm model also can distinguish whether the adsorption was favorable or not by using the dimensionless constant separation factor shown in Eq. 5,

$$R_L = \frac{1}{1 + K_L C_0} \quad (5)$$

where K_L is the Langmuir constant and C_0 is the initial adsorbate concentration. The adsorption is unfavorable if the R_L value is greater than 1. However, if the value of R_L is between 1 and 0, then the adsorption is favorable. The adsorption is linear if $R_L = 1$.

All fitting parameters obtained from Fig. 5 are summarized in Table 2. The coefficients of determination for the Langmuir isotherm model (Table 2) were much higher than those for the Freundlich isotherm model, indicating that the adsorption of Pb(II) and Fe(III) ions followed the Langmuir isotherm model (Eq. 4) because the Pb and Fe ions were equally and homogeneously spread over the cell-o-PDAm porous surfaces. The separation factor R_L , which was calculated for various amounts of adsorbents for cell-o-PDAm, was $0 < R_L < 1$ (Table 2).

The R values were much smaller than 1, indicating a high affinity of cell-o-PDAm for Pb(II) and Fe(III).

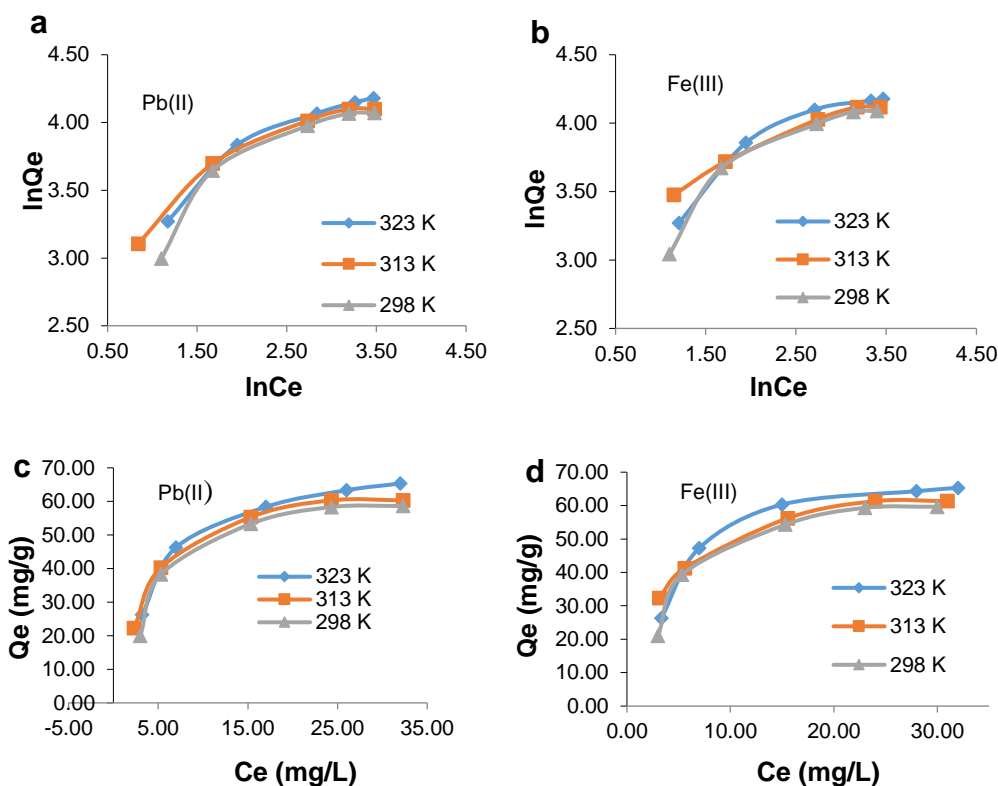


Fig. 5. Langmuir of (a) Pb(II) and (b) Fe(III); Freundlich adsorption model of (c) Pb(II) and (d) Fe(III) ions on cell-o-PDAm at various temperatures

Table 2. Langmuir and Freundlich Parameters for the Adsorption of Pb(II) and Fe(III) Ions by cell-o-PDAm

		Fe(III)			Pb(II)		
Temperature (K)		298	313	323	298	313	323
Langmuir Isotherm	Q^0 (mg/g)	2.3792	2.7137	2.6616	2.3873	2.1645	2.3873
	K_L (L/mg)	0.1540	0.1259	0.1274	0.1050	0.1112	0.105
	R_L	0.01282	0.01563	0.01545	0.01869	0.01754	0.01869
	R^2	0.8705	0.9176	0.9178	0.9607	0.8771	0.967
Freundlich Isotherm	$1/n$	0.9016	0.6095	0.8466	0.9108	0.7149	0.824
	K_F (L/mg)	21.3427	29.7967	24.229	20.4750	26.222	24.366
	R^2	0.9507	0.995	0.9543	0.945	0.9867	0.9762

Kinetics Adsorption

The two kinetic models, pseudo-first-order (Eq. 7) and pseudo-second-order (Eq. 8), were used to describe the kinetics of the adsorption process, comprising the adsorption rates and adsorption mechanism of the metal ions Pb(II) and Fe(III) onto the surface of cell-o-PDAm (Zhao *et al.* 2014; Jodeh *et al.* 2016):

$$\ln(q_e - q_t) = \ln q_e - K_1 t \quad (7)$$

$$\frac{t}{q_t} = \frac{1}{k_2 q_e^2} + \frac{t}{q_e} \quad (8)$$

In addition, the intraparticle diffusion model (Eq. 9) was used to determine the rate-determining step during the metal ion adsorption,

$$Q_t = K_{id}t^{\frac{1}{2}} + Z \quad (9)$$

where Q_e and Q_t are the adsorption capacities at equilibrium (mg/g), t is the various times (min), K_1 is the pseudo-first-order rate constant (1/min), K_2 is the pseudo-second-order rate constant (g/mg min), K_{id} is the intraparticle diffusion rate constant (mg/gmin^{1/2}), and Z (mg/g) was used to conclude the thickness of the boundary layer.

Additionally, the liquid film diffusion model (Eq. 10) was employed to investigate whether the transport of metal ions from the liquid phase to the solid phase boundary plays a role in the adsorption process,

$$\ln(1 - F) = -K_f t \quad (10)$$

where F is the fractional attainment of equilibrium ($F = q_t/q_e$), q_e is the adsorption capacity of the sorbent at equilibrium (mg×g⁻¹), and K_f is the liquid film diffusion constant. A linear plot of $\ln(1 - F)$ versus t with zero intercept would suggest that the kinetics of the adsorption process was controlled by diffusion from the liquid surrounding the solid sorbent.

The values of all the parameters shown in the above equations are summarized in Table 3 and Fig. 5.

Table 3A. The Pseudo-second-order Model for Adsorption of Pb(II) and Fe(III) ions by Cell-o-PDAm

T (K)	298			313			323		
	K_2 (g/mg × min)	Q_{cal} (mg/g)	R^2	K_2 (g/mg × min)	Q_{cal} (mg/g)	R^2	K_2 (g/mg × min)	Q_{cal} (mg/g)	R^2
Fe(III)	0.3568	416.5	0.9868	0.3911	533.5	0.97 45	0.3814	622.8	0.9845
Pb(II)	0.3568	152.9	0.9866	0.3907	196.3	0.97 48	0.3813	230.7	0.9836

Table 3B. The Intraparticle Diffusion Parameters of Pb(II) and Fe(III) ions onto Cell-o-PDAm

T (K)	298			313			323		
	K_{id}	Z	R^2	K_{id}	Z	R^2	K_{id}	Z	R^2
Fe(III)	1.041	1.92	0.931	1.126	1.851	0.905	1.333	1.689	0.944
Pb(II)	0.905	1.08	0.934	1.036	0.871	0.942	1.083	0.96	0.963

The value of K_1 was obtained by plotting $\ln(q_e - q_t)$ vs. t (Fig. S3a), while the K_2 values and the adsorption capacity q_e were calculated from the slope and the intercept of plotting t/q_t vs. t (Fig. S3b). The values for K_{id} and Z were obtained from plotting q_t vs. $t^{1/2}$ (Fig. S3c). When the experimental data was plotted for both the pseudo-first-order and the second-pseudo-order kinetics, the coefficients of determination (R^2) for the pseudo-second-order (0.91 to 0.973) were higher than the pseudo-first-order (0.891). The

calculated q_e values (2.675 mg/g, 15.252 mg/g, and 20.856 mg/g) for the pseudo-second-order (see Table 3 and Fig. S3c) were close to the experimental q_e values (2.133 mg/g, 13.91 mg/g, and 18.786 mg/g), indicating that the adsorption process of metal ions on the surfaces of cell-o-PDAm followed the pseudo-second-order.

All plots shown in Fig. S3 did not pass through the origin, indicating the presence of more than one rate-determining step in the absorption processes. From the initial linearity of the graphs shown in Fig. S3c, the adsorption process of Pb(II) and Fe(III) ions occurred first *via* an instant adsorption stage (on the exterior surface of cell-o-PDAm), which may have resulted in a chemical complexation between the metal ions, amines, and other functionalities (Guo *et al.* 2008). Additionally, the rest of the stages were linear, indicating the gradual adsorption and the intraparticle diffusion rate limiting step of Pb(II) and Fe(III) ions. The values of Z in Table 3 indicate an expansion in the surface layer and a diminished external mass transfer while the potential for internal mass transfer increased.

The mechanism for the removal of metals *via* adsorption occurred in several steps. In the first step, the metal ions migrate from the solution to the external surface of the adsorbent. This was followed by the diffusion through the boundary layer to the active sites. Finally, intraparticle diffusion and the adsorption of metal ions in the inner part of the polymer occurred. The valid mechanism in this work was examined by the two models: the liquid-film model and the intraparticle-diffusion model. The liquid-film diffusion model (Eq. 10) assumed that the flow of the adsorbate molecules through a liquid film surrounding the adsorbent was the rate-determining step. According to Eq. 10, a linear plot of $-\ln(1 - F)$ vs. t (Fig. 6) with a zero intercept suggested that the kinetics of the adsorption process were controlled by diffusion through the surrounding liquid film. As shown in Fig. 6, the experimental adsorption data of the metals by cell-o-PDAm from an aqueous solution at different temperatures did not provide straight lines that passed through the origin, and had coefficients of determination 0.1876 and 0.1578 for Fe(III) and Pb(II) (Table 5), respectively. This indicated that the diffusion of the metals through the liquid film around the cellulose-amine was not the rate-determining step, but may contribute to the adsorption process, especially at the beginning of the adsorption as shown in Table 3.

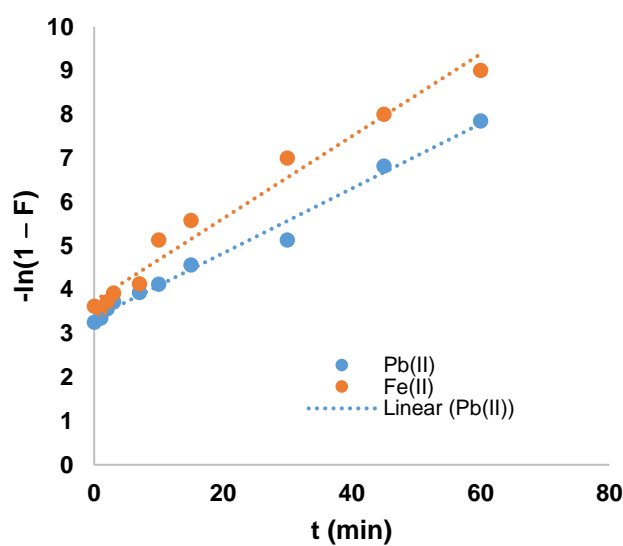


Fig. 6. Liquid film diffusion model plots for the adsorption of composite based of cellulose

Table 4. Liquid Film Diffusion Model Parameters

	K_{df}	R^2
Fe(II)	0.1876	0.9735
Pb(II)	0.1578	0.9873

Adsorption Thermodynamics

The Gibbs free energy (ΔG_0), enthalpy (ΔH_0), and entropy (ΔS_0) were calculated according to the following equations and the results are summarized in Table 5. These are important when evaluating the behavior of the adsorption of Pb(II) and Fe(III) ions on cell-o-PDAm. The equations are as follows,

$$K_c = \frac{C_{ads}}{C_e} \quad (11)$$

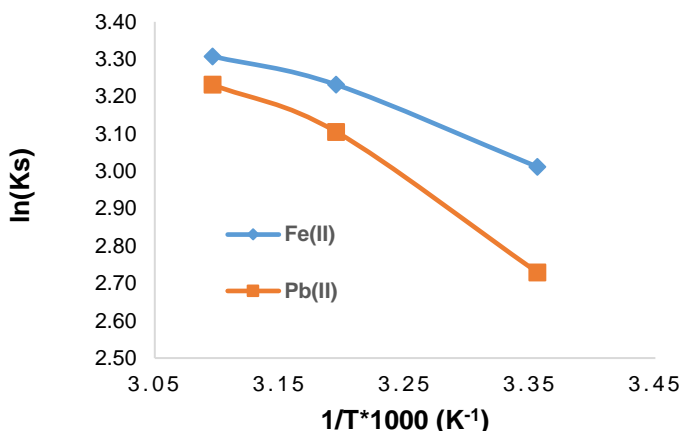
$$\Delta G^\circ = -RT \ln K_c \quad (12)$$

$$\ln K_s = \frac{\Delta S}{R} - \frac{\Delta H}{RT} \quad (13)$$

where K_c is an apparent constant of the thermodynamics, C_{ads} is the amount adsorbed at equilibrium (mg/L), C_e is the equilibrium concentration in an aqueous solution of metal ion (mg/L), R is the gas constant (J/mol \times K), and T is the ions solution temperature (K) (Azzaoui and Mejdoubi 2014).

Table 5. Thermodynamic Parameters for the Adsorption of Pb(II) and Fe(III) ions onto Cell-o-PDAm

T(K)	Fe(III)			Pb(II)		
	ΔG° (KJ/mol)	ΔH° (KJ/mol)	ΔS° (J/K.mol)	ΔG° (KJ/mol)	ΔH° (KJ/mol)	ΔS° (KJ/mol)
298	-17.144	9.66368	57.5627	-18.6156	16.4161	77.9326
313	-17.0074			-19.5535		
323	-18.5832			-20.1787		

**Fig. 7.** Adsorption thermodynamics of Pb(II) and Fe(III) ions by cell-o-PDAm

The K_c value was calculated according to the Van't Hoff equation (Eq. 11) (Zhang *et al.* 2010). The standard Gibbs free energy (ΔG_0) (Jmol^{-1}) was calculated using Eq. 12. The $\ln(K_s)$ versus $1/T$ was plotted as shown in Fig. 7. The slopes and the intercept were used to calculate various thermodynamics parameters; results are shown in Table 5. The obtained values of ΔS_0 and ΔH_0 were positive, while the entropy increased at the solid/solution interface, driven by the adsorption process. The free energies were negative, indicating a spontaneous adsorption process at the tested temperatures.

CONCLUSIONS

1. Cellulose powder derivatized with an aromatic amine chelating agent (cell-o-PDAm) was successfully prepared from cellulose powder extracted from olive industry solid waste.
2. The efficiency of the prepared cell-o-PDAm toward adsorbing the metal ions Fe(III) and Pb(II) was studied as a function of adsorbent dose, temperature, pH, metal ion initial concentration, and time.
3. The cell-o-PDAm polymer showed an excellent efficiency toward both metals, the highest absorbency was observed at a pH of approximately 8.0 and at room temperature.
4. The polymer showed excellent efficiency for metal ions present in a real sample of sewage.
5. The kinetic study revealed that the metal ion adsorption by cell-o-PDAm was pseudo-second-order and followed the Langmuir isotherm model.
6. The thermodynamic analysis showed a negative free energy, indicating a spontaneous adsorption process at different temperatures.

ACKNOWLEDGEMENTS

The authors want to thank the Palestinian Ministry of Higher Education for their financial support of this work. The authors want to acknowledge the An-Najah National University in Palestine for Polymer Metal and Polymer Analysis.

REFERENCES CITED

- Abdel-Ghani, N. T., Hefny, M., and El-Chaghaby, G. A. F. (2007). "Removal of lead from aqueous solution using low cost abundantly available adsorbents," *International Journal of Environmental Science and Technology* 4(1), 67-73.
- Acar, F. N., and Eren, Z. (2006). "Removal of Cu(II) ions by activated poplar sawdust (Samsun clone) from aqueous solutions," *Journal of Hazardous Materials* 137(2), 909-914. DOI: 10.1016/j.hazmat.2006.03.014
- Adeyemo, A. A., Adeoye, I. O., and Bello, O. S. (2017). "Adsorption of dyes using different types of clay: A review," *Applied Water Science* 7(2), 543-568. DOI: 10.1007/s13201-015-0322-y

- Algarra, M., Bartolić, D., Radotić, K., Mutavdžić, D., Pino-González, M. S., Rodríguez-Castellón, E., Lázaro-Martínez, J. M., Guerrero-González, J. J., Esteves da Silva, J. C. G., and Jiménez-Jiménez, J. (2019). "P-doped carbon nano-powders for fingerprint imaging," *Talanta* 194, 150-157. DOI: 10.1016/j.talanta.2018.10.033
- Azzaoui, K., and Mejdoubi, E. (2014). *Elaboration and Study of Some Composites Based on Phosphocalcic Hydroxyapatite, Intended for Industrial and Medical Uses*, Faculty of Sciences, Mohamed 1st University, Oujda, Morocco.
- Bo, S., Ren, W., Lei, C., Xie, Y., Cai, Y., Wang, S., Gao, J., Ni, Q., and Yao, J. (2018). "Flexible and porous cellulose aerogels/zeolitic imidazolate framework (ZIF-8) hybrids for adsorption removal of Cr(IV) from water," *Journal of Solid State Chemistry* 262, 135-141. DOI: 10.1016/j.jssc.2018.02.022
- Chwastowski, J., Staroń, P., Kołoczek, H., and Banach, M. (2017). "Adsorption of hexavalent chromium from aqueous solutions using Canadian peat and coconut fiber," *Journal of Molecular Liquids* 248, 981-989. DOI: 10.1016/j.molliq.2017.10.152
- Doan, H. D., Lohi, A., Dang, V. B. H., and Dang-Vu, T. (2008). "Removal of Zn⁺² and Ni⁺² by adsorption in a fixed bed of wheat straw," *Process Safety and Environmental Protection* 86(4), 259-267. DOI: 10.1016/j.psep.2008.04.004
- Guo, X., Zhang, S., and Shan, X. Q. (2008). "Adsorption of metal ions on lignin," *Journal of Hazardous Materials* 151(1), 134-142. DOI: 10.1016/j.jhazmat.2007.05.065
- Gupta, V. K., Nayak, A., and Agarwal, S. (2015). "Bioadsorbents for remediation of heavy metals: Current status and their future prospects," *Environmental Engineering Research* 20(1), 1-18. DOI: 10.4491/eer.2015.018
- Gupta, S., and Babu, B. V. (2009). "Utilization of waste product (tamarind seeds) for the removal of Cr(VI) from aqueous solutions: Equilibrium, kinetics, and regeneration studies," *Journal of Environmental Management* 90(10), 3013-3022. DOI: 10.1016/j.jenvman.2009.04.006
- Hamed, O., Fouad, Y., Hamed, E. M., and Al-Hajj, N. (2012). "Cellulose powder from olive industry solid waste," *BioResources* 7(3), 4190-4201. DOI: 10.15376/biores.7.3.4190-4201
- Hamed, O., Jodeh, S., Al-Hajj, N., Abo-Obeid, A., Hamed, E. M., and Fouad, Y. (2014). "Cellulose acetate from biomass waste of olive industry," *Journal of Wood Science* 61(1), 45-62. DOI: 10.1007/s10086-014-1442-y
- Heinze, T., and Liebert, T. (2001). "Unconventional methods in cellulose functionalization," *Progress in Polymer Science* 26(9), 1689-1762. DOI: 10.1016/S0079-6700(01)00022-3
- Hokkanen, S., Bhatnagar, A., and Sillanpa, M. (2016). "A review on modification methods to cellulose-based adsorbents to improve adsorption capacity," *Water Research* 91, 156-173. DOI: 10.1016/j.watres.2016.01.008
- Jodeh, S., Amarah, J., Radi, S., Hamed, O., Warad, I., Salghi, R., Chetouni, A., Samhan, S., and Alkowni, R. (2016). "Removal of methylene blue from industrial wastewater in Palestine using polysiloxane surface modified with bipyrazolotripodal receptor," *Morocco Journal of Chemistry* 4(1), 140-156.
- Jodeh, S., Hamed, O., Melhem, A., Salghi, R., Jodeh, D., Azzaoui, K., Benmassaoud, Y., and Murtada, K. (2018). "Magnetic nanocellulose from olive industry solid waste for the effective removal of methylene blue from wastewater," *Environmental Science and Pollution Research* 25(22), 22060-22074. DOI: 10.1007/s11356-018-2107-y

- Karnitz, Jr., O., Gurgel, L. V. A., De Melo, J. C. P., Botaro, V. R., Melo, T. M. S., De Freitas Gil, R. P., and Gil, L. F. (2007). "Adsorption of heavy metal ion from aqueous single metal solution by chemically modified sugarcane bagasse," *Bioresource Technology* 98(6), 1291-1297. DOI: 10.1016/j.biortech.2006.05.013
- Kim, U. J., Kuga, S., Wada, M., Okano, T., and Kondo, T. (2000). "Periodate oxidation of crystalline cellulose," *Biomacromolecules* 1(3), 488-492. DOI: 10.1021/bm0000337
- Lázaro-Martínez, J. M., Romasanta, P. N., Chattah, A. K., and Buldain, G. Y. (2010). "NMR characterization of hydrate and aldehyde forms of imidazole-2-carboxaldehyde and derivatives," *The Journal of Organic Chemistry* 75(10), 3208-3213. DOI: 10.1021/jo902588s
- Limousin, G., Gaudet, J. P., Charlet, L., Szenknect, S., Barthès, V., and Krimissa, M. (2007). "Sorption isotherms: A review on physical bases, modeling and measurement," *Applied Geochemistry* 22(2), 249-275. DOI: 10.1016/j.apgeochem.2006.09.010
- Lin, J., Chen, X., Chen, C., Hu, J., Zhou, C., Cai, X., Wang, W., Zheng, C., Zhang, P., Cheng, J., *et al.* (2018). "Durably antibacterial and bacterially anti-adhesive cotton fabrics coated by cationic fluorinated polymers," *ACS Applied Materials & Interfaces* 10(7), 6124-6136. DOI: 10.1021/acsami.7b16235
- Liu, B., Wang, D., Yu, G., and Meng, X. (2013). "Removal of F⁻ from aqueous solution using Zr(IV) impregnated dithiocarbamate modified chitosan beads," *Chemical Engineering Journal* 228, 224-231. DOI: 10.1016/j.cej.2013.04.099
- Milieu Ltd., WRc, and Risk & Policy Analysts Ltd. for the European Commission (2010). "Environmental, economic and social impacts of the use of sewage sludge on land," (http://ec.europa.eu/environment/waste/sludge/pdf/part_iii_report.pdf), Accessed 02 Aug 2011.
- Moa, J., Yanga, Q., Zhang, N., Zhang, W., Zheng, Y., and Zhang, Z. (2018). "Review on agro-industrial waste (AIW) derived adsorbents for water and wastewater treatment," *Journal of Environmental Management* 227, 395-405. DOI: 10.1016/j.jenvman.2018.08.069
- Muhammad, R. R., Nor, A. Y., Mohammad, J. H., Norazowa, I., Faruq, M., Sazlinda, K., and Hamad, A. A.-L. (2018). "Iminodiacetic acid modified kenaf fiber for waste water treatment," *International Journal of Biological Macromolecules* 112, 754-760. DOI: 10.1016/j.ijbiomac.2018.02.035
- Nada, A. M. A., Eid, M. A., El Bahnasawy, R. M., and Khalifa, M. N. (2002). "Preparation and characterization of cation exchangers from agricultural residues," *Journal of Applied Polymer Science* 85(4), 792-800. DOI: 10.1002/app.10647
- Nagy, B., Maicaneanu, A., Indolean, C., Burca, S., Silaghi, L., and Majdik, C. (2013). "Cadmium (II) ions removal from aqueous solutions using Romanian untreated fir tree sawdust – A green biosorbent," *Acta Chimica Slovenica* 60(2), 263-273.
- O'Connell, D. W., Birkinshaw, C., and O'Dwyer, T. F. (2008). "Heavy metal adsorbents prepared from the modification of cellulose: A review," *Bioresource Technology* 99(15), 6709-6724. DOI: 10.1016/j.biortech.2008.01.036
- Qaiser, S., Saleemi, A. R., and Umar, M. (2009). "Biosorption of lead from aqueous solution by *Ficus religiosa* leaves: Batch and column study," *Journal of Hazardous Materials* 166(2-3), 998-1005. DOI: 10.1016/j.ijhazmat.2008.12.003

- Sahmoune, M. N., Louhab, K., and Boukhiar, A. (2011). "Advanced biosorbents materials for removal of chromium from water and wastewaters," *Environmental Progress & Sustainable Energy* 30(3), 284-293. DOI: 10.1002/ep.10473
- Saravanan, R., and Ravikumar, L. (2015). "The use of new chemically modified cellulose for heavy metal ion adsorption and antimicrobial activities," *Journal of Water Resource and Protection* 7(6), 530-545. DOI: 10.4236/jwarp.2015.76042
- Sud, D., Mahajan, G., and Kaur, M. P. (2008). "Agricultural waste material as potential adsorbent for sequestering heavy metal ions from aqueous solutions – A review," *Bioresource Technology* 99(14), 6017-6027. DOI: 10.1016/j.biortech.2007.11.064
- Uddin, M. K. (2017). "A review on the adsorption of heavy metals by clay minerals, with special focus on the past decade," *Chemical Engineering Journal* 308, 438-462. DOI: 10.1016/j.cej.2016.09.029
- Vieira, M.G. A., De Almeida Neto, A. F., Da Silva, M. G. C., Carneiro, C.N., and DeMelo Filho, A. A. (2014). "Adsorption of lead and copper ions from aqueous effluents on rice husk ash in a dynamic system," *Brazilian Journal of Chemistry Engineering* 31(2), 519-529. DOI: 10.1590/0104-6632.20140312s00002103
- Zelić, E., Vuković, Z., and Halkijević, I. (2018). "Application of nanotechnology in wastewater treatment," *Građevinar* 70(4), 315-323. DOI: 10.14256/JCE2165.2017
- Zhang, Z., Li, M., Chen, W., Zhu, S., Liu, N., and Zhu, L. (2010). "Immobilization of lead and cadmium from aqueous solution and contaminated sediment using nanohydroxyapatite," *Environmental Pollution* 158(2), 514-519. DOI: 10.1016/j.environpol.2009.08.024
- Zhao, X., Wang, W., Zhang, Y., Wu, S., Li, F., and Liu, J. P. (2014). "Synthesis and characterization of gadolinium doped cobalt ferrite nanoparticles with enhanced adsorption capability for Congo Red," *Chemical Engineering Journal* 250, 164-174. DOI: 10.1016/j.cej.2014.03.113

Article submitted: March 26, 2019; Peer review completed: June 3, 2019; Revised version received: June 8, 2019; Accepted: June 10, 2019; Published: June 19, 2019. DOI: 10.15376/biores.14.3.6247-6266

APPENDIX

Supplementary Information

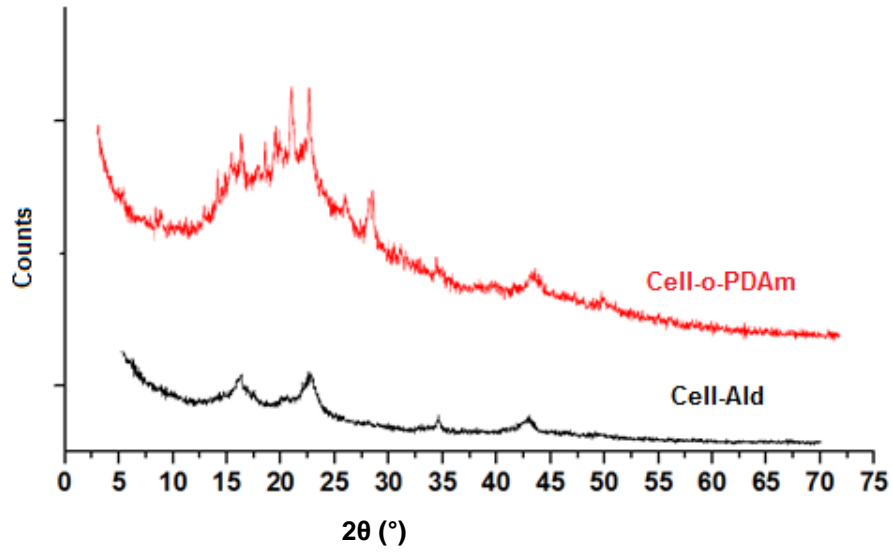


Fig. S1. XRD spectra of cellulose aldehyde and cell-o-PDAM

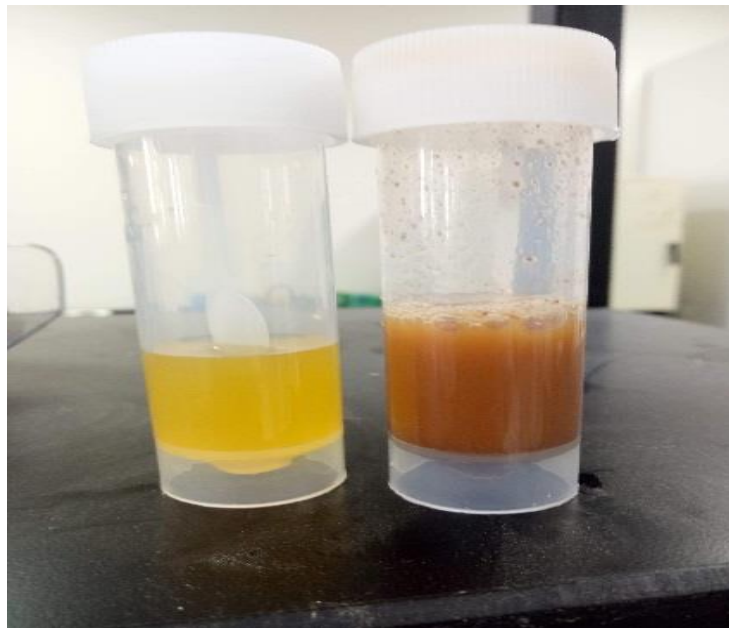


Fig. S2. Images of wastewater sample before and after treatment with cell-o-PDAM

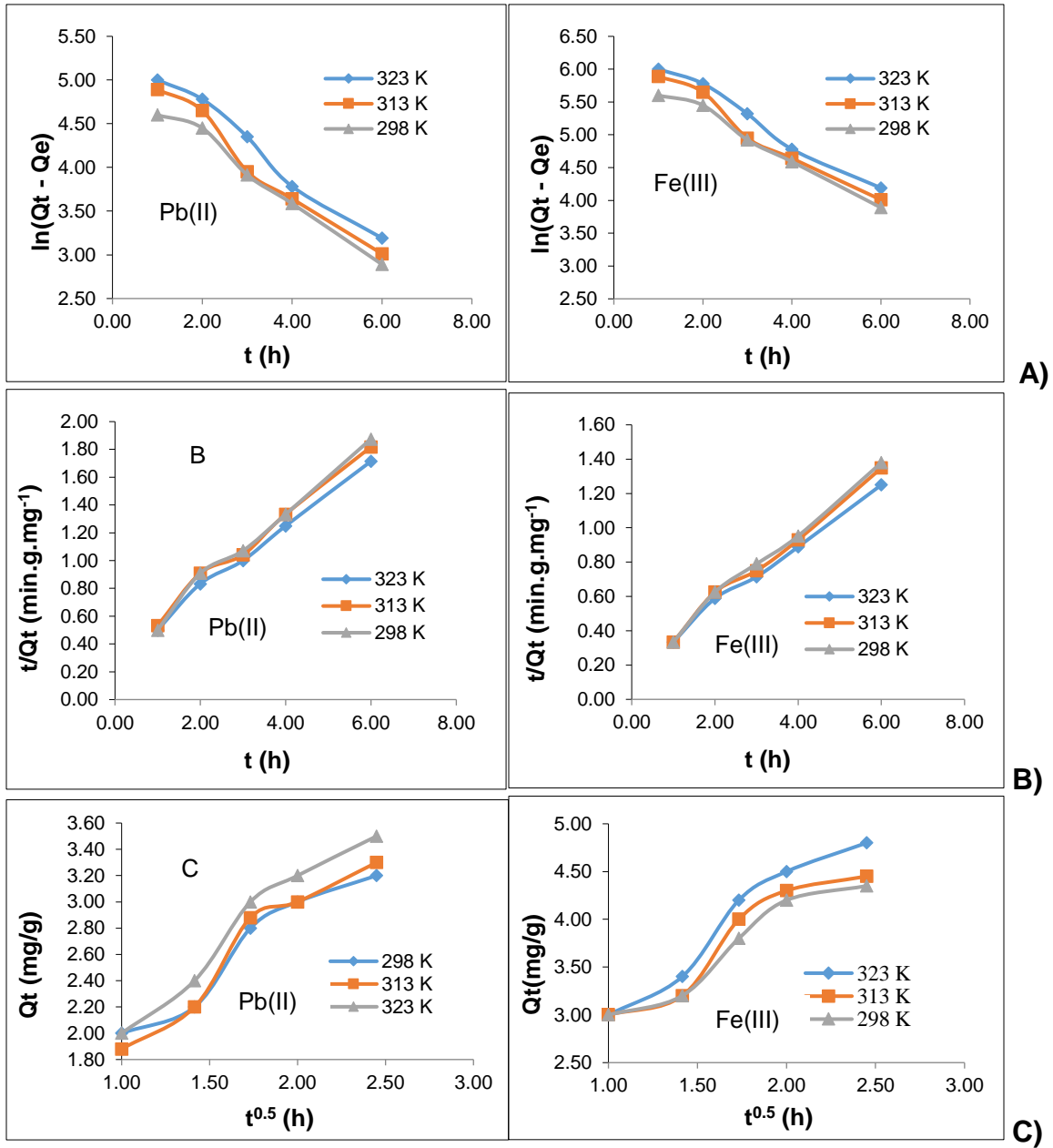


Fig. S3. A) Pseudo-first-order model for the adsorption of Pb(II) and Fe(III); B) Pseudo-second-order model for the adsorption of Pb(II) and Fe(II) ions by cell-o-PDAm; C) Intraparticle diffusion model for the adsorption of Pb(II) and Fe(III) ions by cell-o-PDAm polymer at various concentrations